ISSN 1726-5479

SENSORS & TRANSDUCERS

vol. 113
2/10

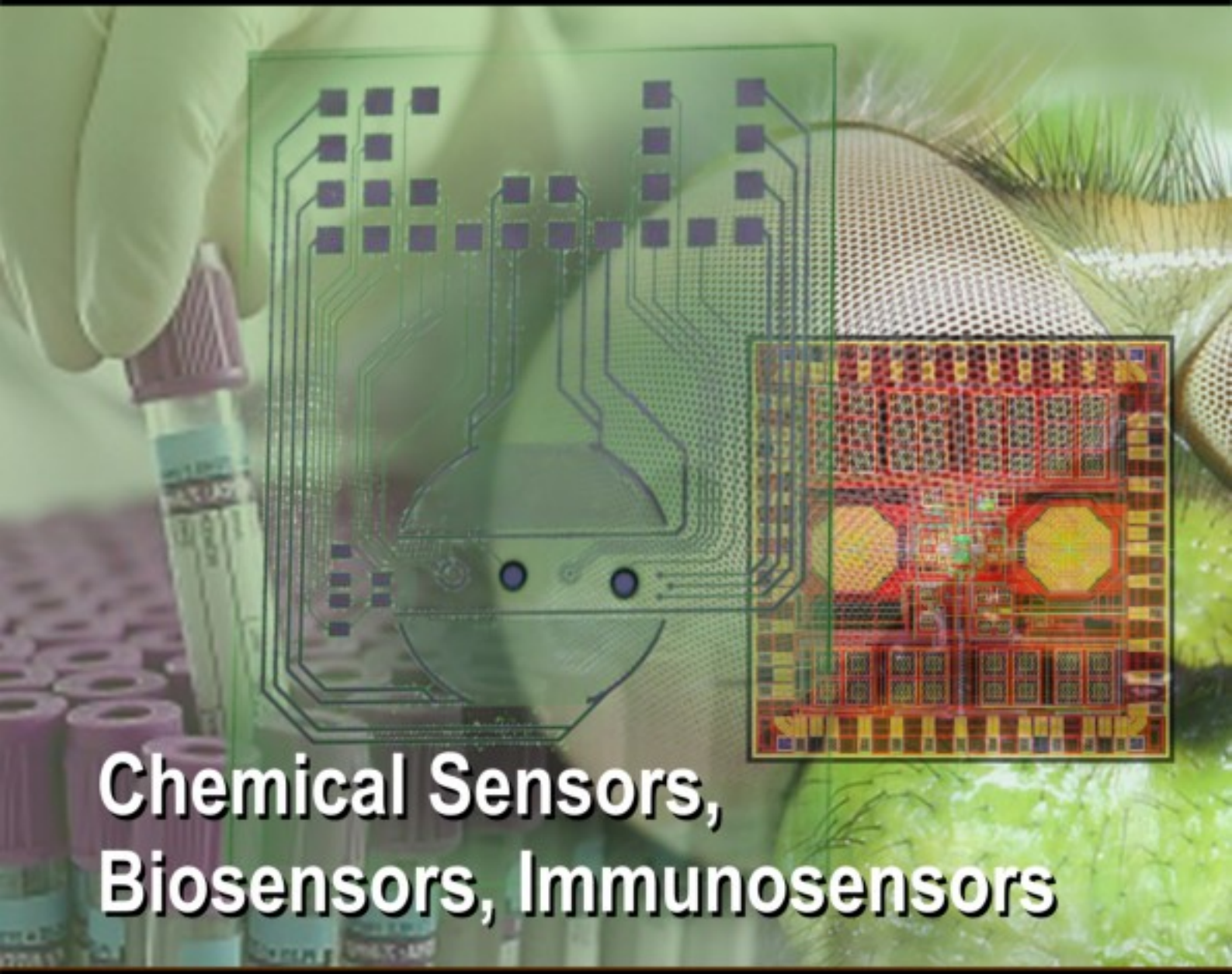

Chemical Sensors, Biosensors, Immunosensors

International Frequency Sensor Association Publishing

IFSA

Sensors & Transducers

Volume 113, Issue 2, February 2010 | **www.sensorsportal.com** | **ISSN 1726-5479**

Sensors & Transducers Journal (ISSN 1726-5479) is a peer review international journal published monthly online by International Frequency Sensor Association (IFSA).
Available in electronic and on CD.

Sensors & Transducers Journal

Contents

Volume 113
Issue 2
February 2010

www.sensorsportal.com

ISSN 1726-5479

Research Articles

Authors are encouraged to submit article in MS Word (doc) and Acrobat (pdf) formats by e-mail: editor@sensorsportal.com
Please visit journal's webpage with preparation instructions: http://www.sensorsportal.com/HTML/DIGEST/Submition.htm

International Frequency Sensor Association (IFSA).

Sensors & Transducers Journal, Vol. 113, Issue 2, February 2010, pp. 18-32

www.sensorsportal.com

Sensors & Transducers

ISSN 1726-5479

http://www.sensorsportal.com

Crossed-Optical-Fiber Oxygen Sensors with Intensity and Temperature Referencing for Use in High-Spatial-Resolution Sensor Arrays

[1]Maria Veronica RIGO, [2]Robert OLSSON and [1]Peter GEISSINGER

[1]University of Wisconsin-Milwaukee, Department of Chemistry & Biochemistry,
3210 N. Cramer Street, Milwaukee, WI 53211-3029, USA

[2]Milwaukee School of Engineering, Department of Physics & Chemistry,
1025 North Broadway, Milwaukee, WI 53202-3109, USA

Fax: (414) 229-5530, tel.: (414) 229-5230

E-mail: geissing@uwm.edu

Received: 23 January 2010 /Accepted: 19 February 2010 /Published: 26 February 2010

Abstract: We investigated the fabrication of an optical-fiber oxygen sensor based on luminescence quenching of a ruthenium (II) complex for our optical-fiber-sensor arrays. Sensor regions are located between two optical fibers forming orthogonal fiber-fiber junctions. Ruthenium molecules are embedded in a photo-polymerized hydrogel matrix, which is covalently attached to the surface-modified fiber-core. For the optical evaluation of these sensors, the fiber sensor junctions are placed in a flow cell. When gaseous oxygen diffuses into the hydrogel, it quenches the luminescence, with the degree of quenching correlating with oxygen partial pressure; this behavior was indeed observed in the crossed-fiber configuration with a sensor response time of 1 s. To account for intensity fluctuations, an oxygen-insensitive dye in an adjacent fiber-fiber junction was used for intensity referencing, which markedly improved the response curves. The oxygen sensor was also corrected for the temperature-dependence of the ruthenium complex using the dye Kiton Red. *Copyright © 2010 IFSA.*

Keywords: Optical fiber, Oxygen sensor, Ruthenium complex, Hydrogel, High-Spatial-Resolution.

1. Introduction

Optical fiber technology in combination with luminescence methods opened a new era of sensors in medical, biological, as well as chemical research. Optical fibers guide light with little loss over

a long distance, which means that source and detection electronics may be located far from the sensor site. This, and the fact that optical fibers are chemically robust platforms for sensors, allows for sensing in challenging environments. Other advantages are, for example, the small footprints of sensors and the relative immunity to electromagnetic interference at the sensor site and along the fiber to and from the sensor site [1]. An important early measuring task considered for optical fiber sensors was the measurement of oxygen in gas phase [2-5], as deficiencies in electrochemical and titration based oxygen sensors, such as slow response time, oxygen consumption and poisoning [6], necessitated finding alternate sensing and transduction modalities. Thus, fiber-optic oxygen sensors based on luminescence measurements have been the subject of research in the past 20 years [7-9]. More than a dozen patents were issued that describe indicators, devices, and procedures for use in liquid or gas phases using excited-state quenching of an appropriate indicator by molecular oxygen. Some of these devices have already been commercialized to monitor oxygen in biomedical or environmental applications [10, 11].

Here, we used our crossed-fiber sensor array architecture to fabricate a ruthenium-based oxygen sensor. The sensor was immobilized in a poly(ethylene glycol) (PEG) matrix. The goal of this work was to determine how the performance of this oxygen sensor integrated in our crossed-fiber sensor architecture compared to existing fiber-optic oxygen sensors, in light of the much smaller probe volume of our sensors. The evaluated parameters were its response time, calibration curves, detection limits, repeatability, and oxygen partial pressure resolution. Furthermore, our fiber architecture allows for placing a second sensor region, e.g., as intensity reference, in close proximity to the principal sensor region for simultaneous monitoring of other parameters of interest. Here we show that using one additional sensor region as an intensity reference greatly enhances the sensor performance and allows for using luminescence intensity changes for optical transduction. Moreover we also have incorporated a temperature-sensitive dye along with the reference dye to correct for the temperaure depencende of the oxygen-sensitive luminophore. Potentially, our sensor architecture also allows for multi-analyte detection, where each sensor region may be sensitive to a different chemical or biochemical species [12].

2. Background

The sensor dyes used here were enclosed in thin hydrogel films, which were covalently attached directly to the fiber core, replacing the original fiber cladding. The refractive index of the PEG cladding was such that the guiding condition of the fiber was maintained, that is, total internal reflection of the light propagating in the fiber core took place at the core/cladding interface. Thus, the interaction of the light propagating in the fiber core, which is used to interrogate the sensor, and the sensor dyes in the cladding was through evanescent fields [13-18]. When light is guided in the core of an optical fiber, a fraction of the radiation extends a short distance from the core into the medium of lower refractive index that surrounds it (*i.e.*, the cladding). This evanescent field, described by Eq. (1), decays exponentially with distance from the core/cladding interface and defines a short-range sensing volume within which the evanescent field may interact with molecular species:

$$E(z) = E_0 \exp(-z / d_p), \tag{1}$$

where $E(z)$ is the evanescent electric field amplitude at distance z from the core/cladding interface, E_0 is the amplitude at this interface. The penetration depth d_p varies for each core mode according to [19]

$$d_p = \frac{\lambda}{2\pi n_{co}\sqrt{(\sin^2\Theta - \sin^2\Theta_z}}, \tag{2}$$

where λ is the free-space wavelength; Θ is the incident angle, which, for guided propagation, is greater than the critical angle Θ_z and n_{co} is the refractive index of the fiber core. Therefore, the range of evanescent fields varies greatly (particularly for the fibers used here, which support many modes); however, the evanescent field ranges relevant for sensing are on the order of one to four times the wavelength of light. Sensor dyes within the range of evanescent fields may absorb light of the appropriate frequency, attenuating the total internal reflection [19]. Also, the luminescence of a sensor dye may be coupled back into a guiding mode of the fiber via the evanescent fields.

The spatial information regarding the location of an emitting luminophore along the fiber can be obtained using optical time-domain reflectometry (OTDR) [20-23] or, more appropriately for luminescence transduction, optical time-of-flight detection (OTOF) [24]. Laser pulses fed into the front end of the fiber cause pulsed evanescent excitation of the luminophores. The luminescence pulses returning to the front end of the fiber arrive with a time delay Δt_d that allows for the calculation of the location L of the emitting luminophore on the fiber according to

$$L = (c / 2n_{co})\Delta t_d \,, \tag{3}$$

where c is the speed of the light. In the case of multi-analyte sensing the spatial resolution, i.e. the minimum separation of adjacent sensor regions, depends upon the luminescence lifetimes of the luminophores. For some sensing tasks, a smaller spacing between adjacent regions is required; in such cases we demonstrated that the use of a second fiber at right angle to the fiber which carries the excitation light pulse (the "excitation fiber") can be employed to provide the time delay necessary to temporally resolve the signals originating at the sensor regions [12, 18, 25]. The second fiber (the "detection fiber"), which provides an optical delay, periodically contacts the first fiber at the sensor regions (see Fig.1). Thus, the emission signal pulse of a luminophore, which is excited through the evanescent fields of the first fiber, is captured by the evanescent fields of the second fiber. With this scheme, even for large numbers of sensor regions, one of the fibers can be very compact, allowing easy handling and monitoring of multiple parameters for a particular location. Earlier, to demonstrate that this architecture allows for arrays containing many sensors, we fabricated a sensor array containing 100 crossed-fiber sensor junctions [12].

If the fiber on which the sensor regions are prepared is used to carry the excitation pulse, the time delay between the excitation of adjacent sensor regions is negligible, but along the detection fiber the sensor regions are spaced much wider, so the return signals are spaced in time accordingly. In this case, the location L along the fiber is given by

$$L = (c / n_{co})\Delta t_d \tag{4}$$

Optical oxygen sensors are commonly based on the ability of molecular oxygen to quench the luminescence of certain transition metal complexes [26] or porphyrin derivates [27]. The variation of the luminescence signal, I (and the luminescence decay time τ) with the oxygen partial pressure, pO_2, is described by the Stern-Volmer equations [28]

$$I_0 / I = 1 + K_{SV} pO_2 \text{ and } \tau_0 / \tau = 1 + K_{SV} pO_2 , \tag{5),(6}$$

where I_0 and τ_0 are the respective luminescence intensity and luminescence lifetime in the absence of oxygen. The Stern-Volmer quenching constant $K_{SV} = k_q \tau_0$ depends on the diffusion-dependent bimolecular quenching constant k_q. The ruthenium complex, $Ru[(Phen)_3]Cl_2$ was chosen for this work as it exhibits high oxygen sensitivity because of its long unquenched lifetime τ_0 (~0.8 μs in ethanolic solution). Furthermore, it absorbs strongly at blue-green wavelengths and has a relatively large Stokes shift. As seen from Eqs. (5) and (6), oxygen pressure may be measured by monitoring luminescence

intensity or luminescence lifetime. We adopted both approaches to compare the intensity-based measurement with intensity referencing to the lifetime measurement. We show that the use of a reference sensor region overcomes many of the problems associated with intensity-based sensors.

3. Experimental

3.1. Probe Preparation

The complex tris (1,10-phenanthroline) ruthenium (II) dichloride (hereafter referred to as "RuPhen"), poly(ethylene glycol) diacrylate (PEG-DA) with an average molecular weight of 575, 2,2-dimethoxy-2-phenylacetophenone (DMPA), 3-(trichlorosilyl) propyl methacrylate (TPM), sulfuric acid (6N), hydrogen peroxide (30% V/V in water) and polyacrylonitrile (PAN) were obtained from Sigma Aldrich Chemical Company (Milwaukee, WI). The reference dye, Rhodamine 110 (Rh110), and the temperature-sensitive dye, Kiton Red (KR, also known as Sulforhodamine B) were purchased from Exciton Corp. Deionized water (resistivity 18 MΩ×cm) was used for the experiments. All reagents were used as received without further purification.

All setups used multimode silica fibers with a TECS (trademark of 3M Corp.) cladding (FT-200-UMT with core diameter of 200 μm) and SMA 905 connectors purchased from ThorLabs, Inc. (Newton, NJ). The fibers had core and cladding refractive indices of n_{co} =1.457 and n_{cl} =1.404, respectively. To use these fibers as sensing platforms, the original fiber cladding has to be removed where the sensors will be located. The original cladding is of insufficient porosity to allow for rapid analyte diffusion into the sensing volume defined by the range of the evanescent fields. Moreover, its chemical composition does not allow for easy encapsulation or attachment of the sensor molecules. Also, a suitable replacement cladding has to be transparent, have a refractive index to maintain the guiding condition of the fiber in the sensor regions, and be compatible with organic and biological media. An excellent candidate for a replacement cladding material is a cross-linked PEG-polymer. The sensor regions themselves were prepared by first removing the fiber jackets of both fibers comprising the fiber junction by mechanical stripping. Subsequently, the cladding layers were removed by rubbing with a cotton swab immersed in acetone and the exposed core was cleaned using Piranha solution (3:1 sulfuric acid:hydrogen peroxide) to eliminate organic residues. The first step in the synthesis of the new cladding was treating the silica core of the fiber with 1M nitric acid solution to activate the hydroxyl groups of the silica. Then, a silanation reaction was carried out by exposing the fiber core surface with a 1 mM solution of TPM in a nitrogen atmosphere, at 18 ^{0}C for 1 hr.[29-31]. The chlorosilane modification of the core is necessary to create gels that adhere covalently to the fiber surface.

The thin PEG-based sensor was synthesized by mixing 1 mL of PEG-DA with 10 mg of DMPA to prepare the PEG-DA precursor solution, which was then diluted with water to make a 40% V/V solution. Separate solutions of 7.0 nM dichlorotris (1,10-phenanthroline) ruthenium (II) complex (i.e., the oxygen sensor dye) and 1.3 nM Rh110 (i.e., the intensity reference dye) were made in ethanol. Each luminophore solution was added to the PEG-DA solution to make a 1:10 (V/V) mixture. Subsequently, the fibers were placed in the flow cell such that orthogonal fiber-fiber junctions were created with the modified fiber cores just touching (see Fig. 1). The first sensor region in the array (i.e., the region that is excited first by the lasere) contains the intensity reference and the temperature sensor dyes (see below). The RuPhen oxygen sensor is located in the second fiber-fiber sensor junction. Once the fiber array is situated inside of the flow cell, 2.0 μL of each luminophore-PEG-DA mixture was placed in the corresponding region using an automatic pipette. The formation of hydrogel microstructure was based upon the UV-initiated free-radical polymerization of methacrylate end groups of the PEG derivatives [32-36] using a Photon Technology International (PTI, Birmingham, NJ) 150-Watt Xenon lamp with a narrow bandpass

interference filter (J43-057 – Edmund Optics). The PEG gel film was cured in ~ 1 minute.

Kiton Red and Rhodamine 110 were independenly encapsulated in polyacrylonitrile (PAN) nanospheres following the procedure reported by Kürner *et al.* [37]. The first sensor region is then formulated by mixing the two dye-loaded PAN nanospheres into the PEG-DA solution to make a 1:10 (V/V) mixture. The 2 μL of this mixture was placed in the first region of the array and UV-cured as described above. Because KR and Rh110 are individually encapsulated within the PAN particles, molecular-level interactions between them are minimized.

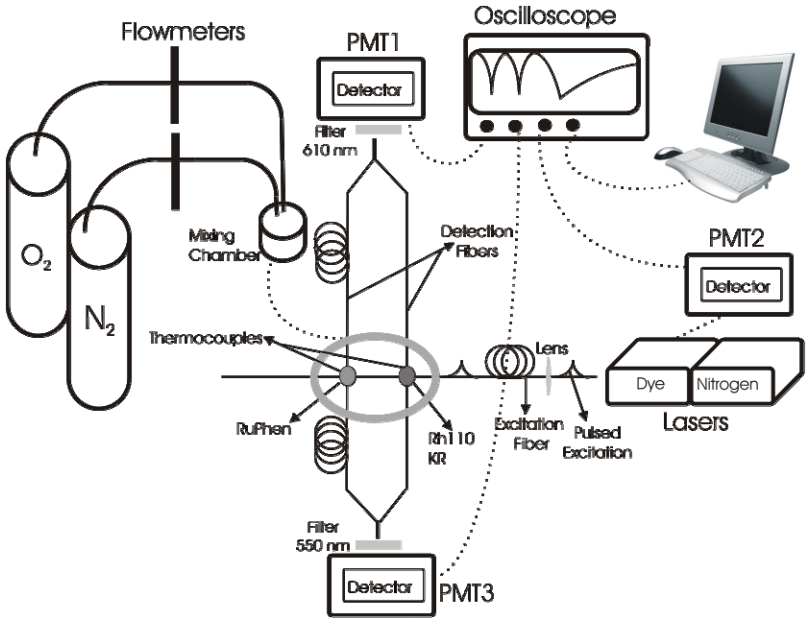

Fig. 1. Experimental setup showing the sensor system.

3.2. Instrumentation

A typical setup used in these experiments is shown in Fig. 1. A dye laser PTI PL201 (using the laser dye Coumarin 460 Exciton Corporation) pumped by a nitrogen laser PTI PL2300 (pulse width 0.6 ns, pulse energy 1.4 mJ, pulse repetition rates of 3-10 Hz) served as the excitation source for the sensor system (465 nm). The sensors were mounted in a home-built flow cell, which could be filled with mixtures of oxygen and nitrogen from pure gas cylinders (Praxair grade 2.6 and 4.8, respectively) at different partial pressures. The gases were premixed in a separate mixing chamber and delivered through 1/4-in.-i.d. flexible PVC tubing into the flow cell.

The luminescence emitted by the sensor molecules was captured by the “detection fibers” and guided to the detector. A 610-nm narrow bandpass filter (NBPF Edmunds NT43-079) was used in front of the Burle C31034A photomultiplier tube (PMT1; with Peltier cooling) to select the RuPhen luminescence and the Rh110 reference pulses. As seen in Fig. 1, the array is designed such that the region containing the reference is excited first; also, the lengths of the detection fibers are chosen such that the emission of the Rh110 reference arrives first at PMT1. The RuPhen luminescence pulse is delayed by passage through an additional stretch of fiber (10 m) to arrive at PMT1 after the reference signal has subsided. Thus, the output current of PMT1, which was analyzed with a LeCroy LC564DL digital storage oscilloscope (DSO) with a bandwidth of 1 GHz and sampling rate of 4 GS/s, displays both sensor signals sequentially in one pulse (usually 1000 averaged traces). A trigger for the DSO was generated using a second PMT2 (RCA 1P28,

1.6-ns rise time), which collected light scattered from the front of the excitation fiber. A LabVIEW (National Instruments) program was written to collect and analyze the data. When testing the temperature effect on the response of the gas-phase oxygen-sensor, the experimental set up shown in Fig. 1 was modified by adding a third photomultiplier tube (PMT3) with a 550-nm NBPF (Edmunds NT43-074) to detect the luminescence of KR, while PMT1 with a 610-nm NBPF can capture the luminescence of Rh110 and RuPhen.

For detailed study of sensor response times, a "smaller setup" was used to eliminate the time needed for the mixture to flow from the mixing chamber through several meters of tubing to the flow cell containing the fiber junction. Instead the fiber junctions were mounted in a PMMA frame, with the junctions suspended in free space over a hole in the mount. The tubing, which was shortened to less than 1 meter, was held directly above the junctions during the measurement, thereby providing a continuous flow of the desired gas mixture. To monitor the temperature during a measurement, a homemade Type K thermocouple (Alumel/Chromel) was placed at the sensor surface inside the flow cell. For cell temperatures above 22 ^{o}C, a temperature controller (Barnstead/Thermolyne Coorporation) regulated the heating of the hot plate, which was in thermal contact with the cell. For lower temperatures, a regular Type K thermocouple mounted to the outside walls of the cell was used to monitor the temperature stability.

4. Results and Discussion

4.1. Quenching Curves

The first experiments employed only the fiber sensor junction containing the RuPhen complex. In these experiments, the gas mixture was allowed to flow through the cell, which was isolated from the environment. The total gas pressure inside the cell was 2.1 atm. These measurements took place at ambient temperature. Changes in the RuPhen luminescence intensity, I, were monitored from a fully nitrogen-saturated atmosphere, I_0, to an environment with increasing oxygen pressures. For each gas mixture, 1000 luminescence pulses were averaged. Luminescence lifetimes were determined from the averaged RuPhen pulse shapes with a single-exponential fit of the trailing part of the RuPhen luminescence pulse. No deconvolution of the signal pulses with the shape of the excitation light pulse had to be carried out. Given the length of fiber (3 m for the excitation fiber and 1 m and 10 m for the detection fibers), the excitation light pulse width at the sensor region is three orders of magnitude smaller than the RuPhen luminescence lifetime, with negligible additional broadening as the luminescence pulse travels to the detector.

To determine the linear dynamic range of the sensor based on the Stern-Volmer model and to determine whether the sensor response deviates from Stern-Volmer behavior, the lifetimes were plotted as (τ_0/τ)-1 vs. pO_2 in Fig. 2a. The inset of this plot displays the averaged pulse traces vs. time; as expected, the pulse intensities decrease with increasing oxygen partial pressure, pO_2, because of non-radiative energy transfer processes from the excited ruthenium complex to molecular oxygen [28]. From a pure nitrogen atmosphere up to 1.5 atm oxygen partial pressure, the measured lifetimes decrease rapidly, however, for oxygen/nitrogen mixtures exceeding 1.5-atm oxygen content, the luminescence lifetimes no longer change significantly with increasing oxygen partial pressure as seen in Fig. 2. One reason for the poor sensitivity in this region is the inherent non-linearity of the Stern-Volmer equations (5) and (6). This is clearly seen from the differential form of the Stern-Volmer equations, e.g., for luminescence lifetimes

$$\frac{d\tau}{d(pO_2)} = \frac{-K_{SV}\tau_0}{(1+K_{SV}pO_2)^2}, \tag{7}$$

which shows that the rate of change of luminescence lifetimes (i.e., the sensitivity) decreases with increasing oxygen partial pressure. The observed changes of the lifetimes also establish the dynamic nature of the quenching process in our system. According to Fig. 2a, the linear response range extends to 1.5 atm oxygen partial pressure. The linear fit of this region using Eq. (6) yields a Stern-Volmer quenching constant of K_{SV} = 0.75 atm^{-1}. This value is comparable to the value of 0.532 atm^{-1} found by Potyrailo *et al*. [38] for oxygen sensing using tetraphenylporphyrin as sensor dye embedded in the crosslinked silicone cladding of an optical fiber. While the silicone cladding is likely to be less porous than PEG hydrogel, the non-polar silicone cladding may facilitate oxygen diffusion leading to large biomolecular quenching constants. It was shown by Mills [39] that efficient diffusion is the most important factor for large values of K_{SV}.

Above pO_2=1.5 atm, deviations from Stern-Volmer behavior occur. As seen in the inset of Fig. 2a, even at these higher oxygen pressures, the averaged signal pulses still exhibit a good signal/noise ratio, meaning that quenching is not complete. This deviation is far stronger than the "negative curvature" observed by others [3, 26, 28, 40]. The porous hydrogel matrix should offer sufficient oxygen permeability at these pressures, however, it is conceivable that adsorption of oxygen to the PEG hydrogel could lead to a smaller local partial pressure [41, 42] at the RuPhen site compared to the external partial pressure. Nevertheless, at higher pressures the sorption-desorption kinetics of oxygen molecules to the hydrogel could be slower than the excited-state deactivation of the immobilized RuPhen complex; thus, the slower the desorption of oxygen, the smaller the number of quencher molecules that will have access to the activated RuPhen [41].

As mentioned above, the trailing edge of the RuPhen signal pulses were well-fitted with a single exponential decay function, with R-values decreasing gradually from R = 0.999 for 0 atm oxygen pressure to R = 0.981 for 2.1 atm oxygen pressure. This is quite useful for sensing purposes, as it allows for easy signal processing and for the construction of calibration curves. There are, however, questions regarding the physical significance of the single lifetimes extracted from this data. First, the disordered structure of the hydrogel implies that the local environments of the sensor dyes show structural variations [43, 44]. This manifests itself in a distribution of excited state lifetimes for any given oxygen partial pressure. These lifetime distributions will affect the observed responses to oxygen exposure as described elsewhere [45-48]. Second, it was demostrated by Kneas *et al.* [49, 50] that micro- and nanocrystallization of the dye molecule in a solid supports can cause non-uniform quenching. As the degree of heterogeneity and microcrystallization increases, the quenching sensitivity decreases and the linearity of the Stern-Volmer model becomes poor. Thus, at higher pO_2 the microcrystal contribution to the emission signal of RuPhen can show apparent oxygen quenching, though the quenching is significantly smaller than the one observed in the bulk polymer matrix. The poor quenching observed at pO_2 higher than 1.5 atm may be due to the presence of highly emissive RuPhen microcrystals in the sensor film. Third, the excitation of the sensor dyes is through exponentially decaying evanescent fields (see Eq. (1)), which means the excitation intensity varies dramatically with distance from the fiber-core surface. Likewise, the sensor luminescence pulses are captured by the detection fiber through these fields, which in this case means that pulses enter the detection fiber with vastly different peak intensities. Thus, it is quite remarkable that the single exponential fit works as well as it does given that the underlying lifetimes and peak intensities are distributed.

Next, we analyzed the dependence of the pulse intensities as a function of oxygen partial pressure. One thousand pulses were averaged for different oxygen partial pressures. The averaged RuPhen signal pulse traces were integrated to determine the pulse areas, *I,* (see Fig. 2b). From a pure nitrogen atmosphere (I_o) to 1.4 atm oxygen partial pressure, the sensor responds rapidly, with a large slope reflecting good sensitivity. For oxygen partial pressures exceeding 1.4 atm, the pulse areas fluctuate significantly with a magnitude much larger than the uncertainties, which are given by the 95% confidence band calculated from the standard deviation of the mean resulting from

averaging three intensity measurements (i.e., N = 3) of 1000 pulses each. We attribute these signal pulse area fluctuations largely to pulse energy fluctuations of the laser light source. These fluctuations, as well as other factors such as photobleaching, probe leaching, as well as changes in the light scattering or absorption characteristics of the sample, are detrimental to measurements where the analyte causes a change in the luminescence intensity of a sensor [52].

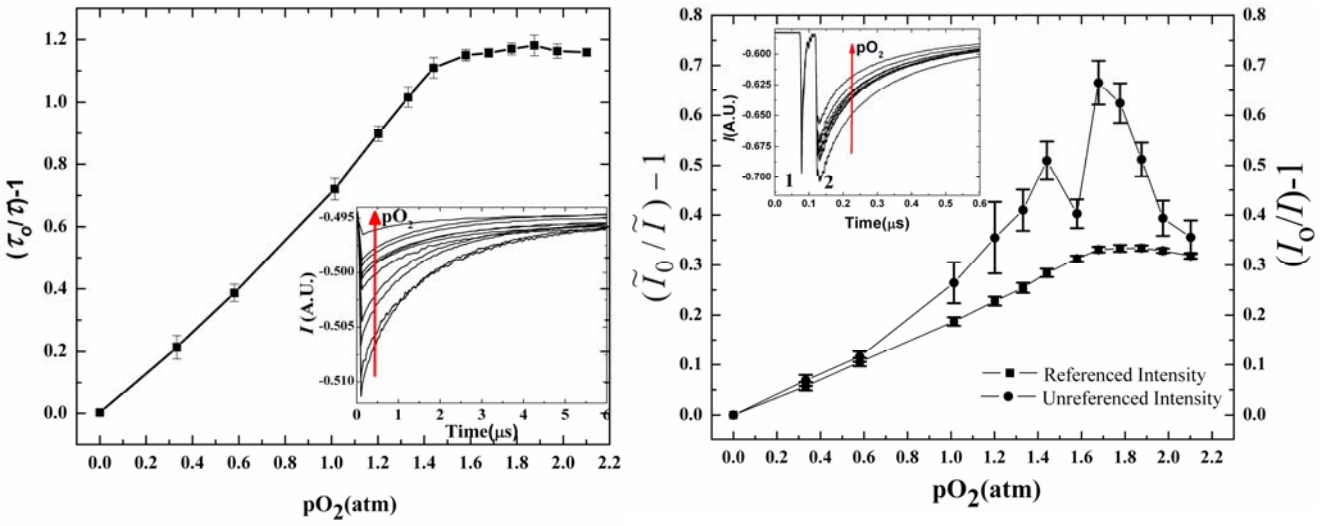

(a) (b)

Fig. 2. (a) Stern-Volmer of the evanescent-based oxygen sensor in terms of RuPhen lifetime. The inset displays the RuPhen pulse traces. **(b)** RuPhen integrated intensity (-●-) and referenced RuPhen integrated intensity(-■-) as function of oxygen partial pressure. The inset displays the pulses traces of Rh110 (1) and RuPhen (2) resolved in time. Error bars for both graphs were calculated using Student's t-value for the 95 % confidence level (N=3).

To compensate for these fluctuations, we employed a second sensor region containing the reference dye, Rh110, which is immune to changes in oxygen pressure and changes in temperature [52]. The experiment is set up such that the signal traces originating at this sensor region (i.e., the first set of peaks in the inset of Fig. 2b) arrive at the detector first, followed by the RuPhen emission. To correct the RuPhen emission intensity for source fluctuations, we divided the averaged integrated intensity of RuPhen by the averaged integrated intensity of Rh110, and plotted this ratio as $(\tilde{I}_0/\tilde{I})$-1 vs. pO_2 (shown in Figure 2b -■-). A clear improvement is seen, as the overall quenching behavior is much more in line with the expected Stern-Volmer behavior (see Eq.(5)) and the high-pressure fluctuations are reduced to the level of the statistical uncertainty. A comparison of the curves in Fig. 2b shows clearly that intensity referencing significantly improves this measurement; the referenced sensor extends the linear dynamic range from approximately 1.33 atm to almost 1.7 atm. The corresponding value using luminescence lifetimes is approximately 1.6 atm (Fig. 2a). Thus, intensity referencing improves the intensity-based linear dynamic range beyond the lifetime-based measurement. This is at first surprising, because the measurement of luminescence lifetimes is intensity-independent, and, therefore, should be superior to measurements based on intensity changes. However, it is likely that as the oxygen partial pressure increases, the description of the multiexponential decay kinetics with single exponential decay is increasingly problematic (as seen by the R-values), limiting the linear response range of the lifetime measurement.

From Fig. 2b the Stern-Volmer constants K_{SV} were determined from the slope in the linear response ranges to be 0.23 atm^{-1} and 0.20 atm^{-1}, with the latter value characterizing the referenced

measurement. Both values are substantially below the value of K_{SV} = 0.75 atm^{-1} extracted from the lifetime measurement. While Eqs. (5) and (6) imply equal Stern-Volmer constants for both lifetime and intensity measurements, it was demonstrated earlier by Lakowicz *et al*. [45] that for systems with distributions of unquenched lifetimes and identical bimolecular quenching constants, $\tau_0/\tau > I_0/I$, just as observed here. As discussed above, broad distributions of the unquenched lifetimes are expected to be present in the disordered PEG cladding. However, the inhomogeneity of dye binding sites on the hydrogel could also lead to differences in the local oxygen-quenching rate constants because of the altered diffusion constants in solid media [39]. From our observation that $\tau_0/\tau > I_0/I$, we conclude that the lifetime distributions are dominant.

To calculate the pressure resolution of our sensor, we use the sensor sensitivity (Eq. (7)) to write

$$\Delta\tau(pO_2) = \left(\frac{d\tau}{d(pO_2)}\right)\Delta pO_2 , \tag{8}$$

where $\Delta\tau(pO_2)$ is measurement uncertainty of the luminescence lifetime at the pressure pO_2, and ΔpO_2 is the corresponding pressure resolution. Using for the luminescence-lifetime uncertainty the 95% confidence band $t \times \sigma_N(\tau)$, *i.e*., the standard deviation of the mean $\sigma_N(\tau)$ at a given pressure with the appropriate t-value for N = 3, we obtain for an oxygen partial pressure of 0.33 atm (close to atmospheric oxygen partial pressure) a sensor resolution of 0.0016 atm. The same calculation for the referenced integrated intensities yields a pressure resolution of 0.0043 atm at a pressure of 0.33 atm. Thus, pressure changes of 0.48% and 1.3% are measureable at this pressurethe with the lifetime and referenced-intensity measurements, respectively. The lifetime measure achieves a slightly better resolution, which is due to the larger Stern-Volmer constant. To calculate the detection limit for oxygen, $pO_2(\min,\tau)$ and $pO_2(\min,\tilde{I})$ we use the sensitivities at pO_2= 0, which are given by

$$d\tau/d(pO_2)\Big|_{pO_2=0} = -K_{SV}\tau_0 \text{ and } d\tilde{I}/d(pO_2)\Big|_{pO_2=0} = -K_{SV}\tilde{I}_0 . \tag{9),(10}$$

We obtain $pO_2(\min,\tau)$ = 0.0012 atm and $pO_2(\min,\tilde{I})$ = 0.0055 atm, respectively. Because of the larger Stern-Volmer constant, the lifetime measurement provides a slightly better detection limit; however, it has to be reemphasized that it is only because of the referencing scheme with a second sensor region that the the detection limts and pressure resolution of intensity-based are almost comparable to the corresponding data obtained from the lifetime-based measurement, Again, these results are based on averaging three luminescence traces of 1000 pulses each; thus, these results may be improved by measurement of additional traces. The oxygen sensor reported by Potyrailo *et al*. [53] used the sensor dye tetraphenylporphyrin, which was allowed to diffuse into the existing silicone cladding of an optical fiber. The oxygen-sensitive section of the fiber extended for 1.5 m; with the low-intensity excitation from an LED, the sensor allowed for a detection limit of 0.004 atm (S/N=3). The O_2-sensor described by Peterson *et al*. [2], which employed the dye perylene dibutyrate contained in an organic polymer adsorbent, offered a pressure resolution of 0.0013 atm. In this case, however, the sensor was located at the distal end of an optical fiber. Thus, in spite of the much smaller sensing volume at the junction of two fibers and in spite of the weak evanescent excitation of the sensor molecules and the evanscent capture of sensor luminescence pulses, our oxygen sensor is comparable to other such sensors reported in the literature.

4.2. Response Time

Because the sensor molecule is contained in a solid matrix, we expect the sensor response time to be influenced by the rate of O_2(g)/N_2(g) diffusion into the film [39, 54]. To reduce the contribution

of the filling-time on the cell and tubing volume to the response time, the "smaller setup" was used (see "Instrumentation" section above). The sensor response time was tested in intensity mode. The regions were initially flushed with a pN_2 of 2.1 atm and the integrated intensity I_0 was determined. Subsequently, the regions were flushed with the desired pO_2/pN_2 mixture. The data was recorded continuously with the gas changing every 100 s. The DSO was set to average only five pulses, which at a typical pulse repetition rate of 5 Hz resulted in a time resolution of 1 s. Each RuPhen data point was divided by the corresponding five-pulse average of Rh110 luminescence pulses. Fig. 3 shows the results for a series of gas mixture composition changes in 100-s intervals. Step-wise oxygen partial pressure changes were carried out from 0 atm pO_2 to 1.97 atm pO_2 and plotted in Fig. 3a, The time resolution is again 1 s. Similar data is shown in Fig. 3b, where large and small pO_2 changes up to 1.97 atm pO_2 were carried out. In all but one case, the sensor response time is less than 1 s; the exception is the change from 0 atm pO_2 to 1.97 atm pO_2 in Fig. 3b, where there was a delay in achieving stable signal levels. It is notable that hysteresis was not observed; particularly returning to a 2.1 atm pN_2 environment reset the sensor signal to the "baseline" level. Given that only five pulses were averaged and that the sensing volume is small, the sensor performance is remarkable. This data also shows that the sensor response time is less than 1 s, which is in agreement with the response time found by McDonagh *et al.* [55] for a ruthenium based oxygen sensor encapsulated in a tetraethoxysilane-based sol-gel film.

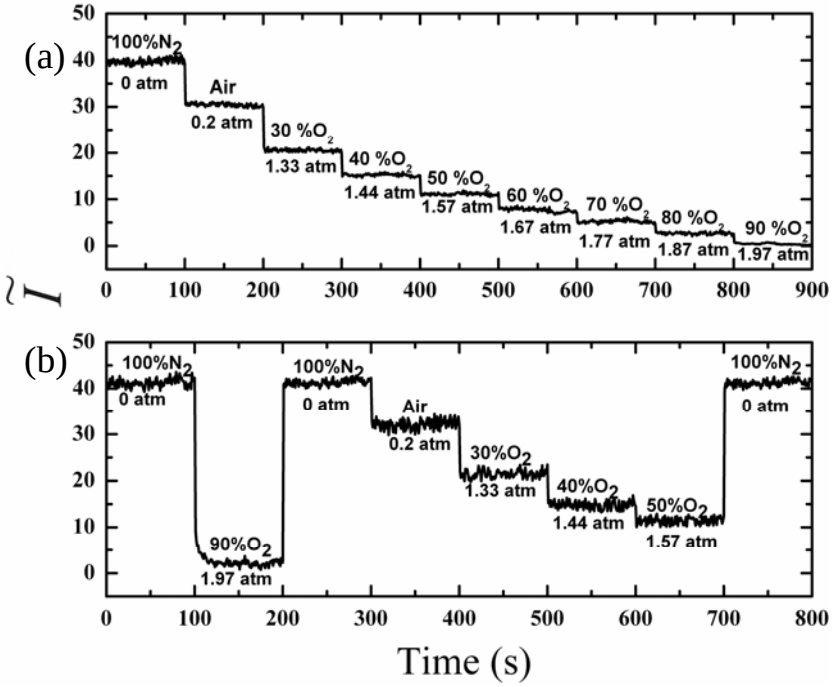

Fig. 3. Sensor response of the oxygen sensor over a pressure range of 0-1.97 atm (a); Sensor response to different oxygen partial pressures showing a good reversibility and reproducibility (b).

It is important to reemphasize that the signal/noise ratio can be improved dramatically by averaging more pulses – the inset of Fig. 2 shows signal pulse traces obtained by averaging 1000 signal pulses. It is apparent that even at maximum quenching (100% pO_2 at 2.1 atm partial pressure) the averaged trace exhibits little noise. The use of light sources with higher pulse-repetition rates allows for averaging more pulses while maintaining the time resolution commensurate with sensor response times.

4.3. Temperature Effects

The parameters that control the overall oxygen sensitivity exhibited by any optical sensor embedded in a polymeric film are provided by the Stern-Volmer constant, $K_{SV} = k_q \tau_0$. In general, the greater the value of K_{SV}, the greater the sensitivity of the optical sensor, thus larger values of k_q and τ_0 are desirable. An increase in temperature will cause a decrease in the natural observed luminophore lifetime, but at the same time it will increase the oxygen diffusion in the matrix. The overall effect of temperature on luminescence intensities and lifetimes can be accounted for by a temperature-dependent Stern-Volmer constant $K_{SV}(T)$ in the Stern-Volmer equations (5) and (6).

One approach to account for the temperature dependence in the measurement of pO_2 is to include in the sensor system a second luminophore that features a temperature-dependent, but oxygen-independent luminescence intensity. A calibration curve for determination of the temperature can be measured by monitoring the emission from the temperature-sensitive luminophore, and then this information can be used to correct the temperature dependence of the oxygen-sensitive luminophore. Kiton Red was chosen as temperature-sensitve dye, because its emission shows a temperature dependence of -1.55 % per ^oC [56]. Using the experimental setup described in Fig. 1, we investigated the effects of temperature on the sensor luminescence between -25 ^oC and 40 ^oC. We compared the temperature-dependence of the luminescence intensity of RuPhen and KR in a 100% pN_2 atmosphere (2.1 atm) and in different pO_2/pN_2 mixtures. Each data point is an average of 10 luminescence traces, each of which consists of 1000 luminescence pulses. Fig. 4 illustrates the temperature dependence of the referenced, integrated emission intensities for RuPhen and KR regions for pressure and temperature ranges of 0-2.1 atm and -25-39 ^oC, respectively.

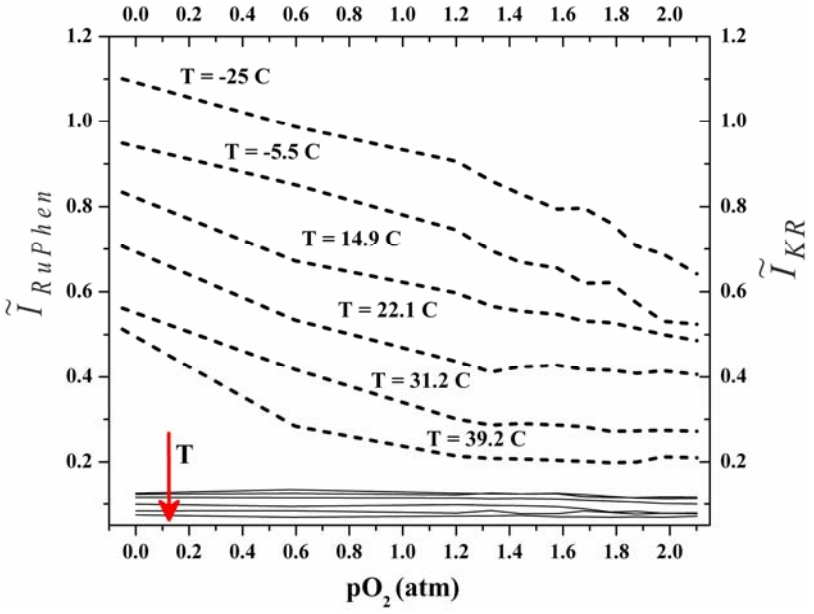

Fig. 4. Referenced intensity of the RuPhen (dashed lines) and the KR (solid lines) as a function of pO_2 at various temperatures. The RuPhen and KR emissions were recorded at the same temperatures.

The pO_2 response of RuPhen as characterized by its quenching efficiency (Q.E.),

$$\text{Q.E.} = [(\tilde{I}_{pO_2=0} - \tilde{I}_{pO_2=2.1atm}) / \tilde{I}_{pO_2=0}] \times 100\% \quad (11)$$

which is strongly temperature dependent: it decreases from 98 % at room temperature to ~ 40% at

-25 ^{o}C, demonstrating again the needed for correcting its response for temperature effects. We measured a temperature dependence of the KR emission of -0.0011% $^{o}C^{-1}$ at pO_2= 2.1 atm and 0.0012% $^{o}C^{-1}$ at pO_2= 0 atm (see Fig. 5a). Thus, the temperature dependence of this dye is nearly independent of pressure, which is a desirable property for a simple temperature correction of the emission intensity-pressure response. We obtained for the temperature dependence (in Kelvin) of the referenced KR intensity the following linear relationship:

$$\tilde{I}_{KR} = 0.44 - 0.0012 \times T(K) \tag{12}$$

This equation allows for measuring the temperature of a particular medium from the referenced KR luminescence intensity. Then calculating K_{SV} from the RuPhen response at different temperatures (using Stern-Volmer curves in Fig. 4) over the oxygen-pressure linear dynamic range, the variation of the Stern-Volmer constant with temperature can be determined. Fig. 5b shows this empirical K_{SV} calibration curve as function of temperature. Fitting a second order polynomial to the K_{SV} vs. T curve yields

$$K_{SV} = -3.05 + 0.027T(K) - 5.44 \times 10^{-5} T^2(K) \tag{13}$$

Eqs. (12) and (13) can now be used to correct the temperature effects on the values of oxygen pressure (using Eq (9)) in a system where the temperature fluctuates.

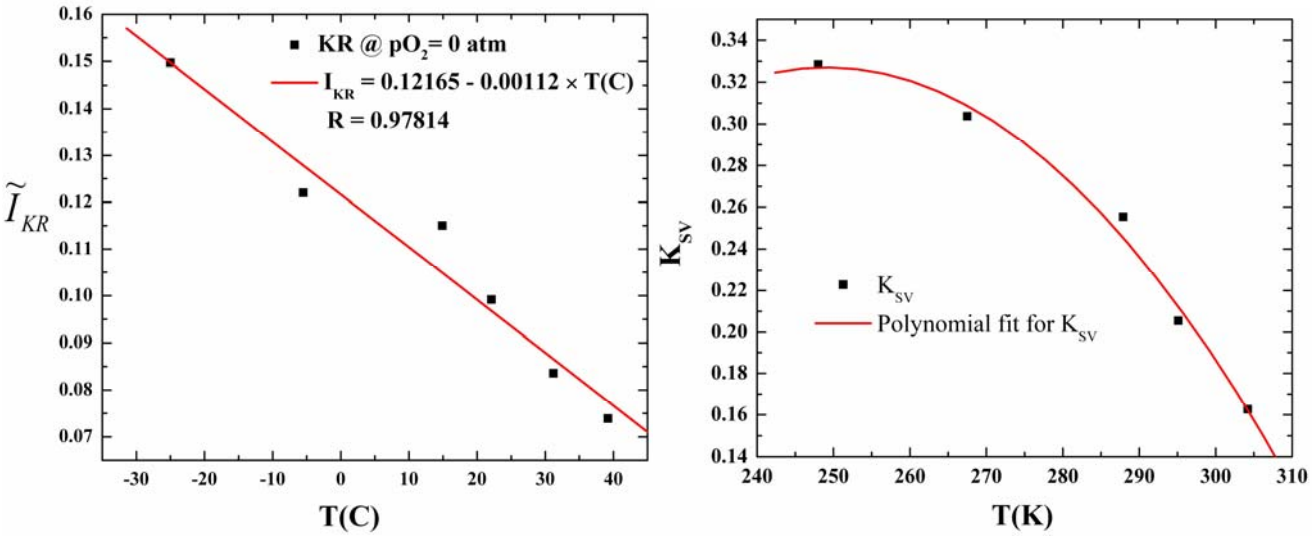

(a) (b)

Fig. 5. Linear regression for the KR referenced intensity as a function of temperature for pO_2=0 atm (a); Variation of K_{SV} as a function of temperature in Kelvin degrees (b).

5. Conclusions

We applied our crossed-fiber sensor array architecture to measure gaseous oxygen using the oxygen-induced quenching of the luminescence of RuPhen. This complex was embedded in a hydrogel, which was covalently attached to the fiber core. Both oxygen-induced changes of the intensity and the luminescence lifetimes were monitored. We showed that both measurements offer similar detection limits and pressure resolution, but only if a second sensor region monitoring the source intensity fluctuations is used a reference for the intensity-based measurement. The sensor

response time is of the order of 1s; the sensor is completely reversible and regenerable, offering excellent repeatability. Because temperature changes affect the oxygen sensor lifetimes and emission intensities a dual-luminophore sensor was developed that enables remote monitoring of the temperature and pressure simultaneously. The calibration curves obtained allowed calculating the K_{SV} for different temperature and thus correct the oxygen partial pressure values obtained with our sensor. The applied corrections of the sensor response for source-intensity fluctuations and for the temperature dependence of the luminescence quenching by using additional crossed-fiber sensor junctions demonstrates the potential of our sensor arrays for multi-analyte and multi-parameter sensing in high-spatial resolution using only two optical fibers.

Acknowledgements

This work was supported by DARPA through the Center for Water Security at the University of Wisconsin-Milwaukee and by a grant from the University of Wisconsin Groundwater Research Program. Support through a University of Wisconsin-Milwaukee Dissertation Fellowship and a Dr. and Mrs. George Sosnovsky Award for Graduate Research (MVR) is gratefully acknowledged. We would like to thank Paul Henning for assistance with data acquisition software.

References

[1]. O. S. Wolfbeis, Fiber-Optic Chemical Sensors and Biosensors, *Anal. Chem.* Vol. 76, 2004, pp. 3269-3284.
[2]. J. I. Peterson, R. V. Fitzgerald, D. K. Buckhold, Fiber-optic probe for in vivo measurement of oxygen partial pressure, *Anal. Chem.* Vol. 56, 1984, pp. 62-67.
[3]. X.-M. Li, K.-Y. Wong, Luminescent platinum complex in solid films for optical sensing of oxygen, *Anal. Chim. Acta,* Vol. 262, No. 1, 1992, pp. 27-32.
[4]. O. S. Wolfbeis, L. J. Weis, M. J. P. Leiner, W. E. Ziegler, Fiber-optic fluorosensor for oxygen and carbon dioxide, *Anal. Chem.,* Vol. 60, No. 19, 1988, pp. 2028-2030.
[5]. A. S. Kocincova, S. M. Borisov, C. Krause, O. S. Wolfbeis, Fiber-Optic Microsensors for Simultaneous Sensing of Oxygen and pH, of Oxygen and Temperature, *Anal. Chem.,* Vol. 79, 2007, pp. 8486-8493.
[6]. L. C. Clark, C. Lyons, Electrode systems for continuous monitoring in cardiovascular surgery, *Annals New York Acad. Sci,* Vol. 102, 1962, pp. 29–45.
[7]. J. N. Demas, B. A. DeGraff, P. B. Coleman, Oxygen Sensors Based on Luminescence Quenching, *Anal. Chem.,* Vol. 71, 1999, pp. 793A-800A.
[8]. G. Orellana, D. García-Fresnadillo, M. D. Marazuela, M. C. Moreno-Bondi, J. Delgado, J. M. Sicilia, In Monitoring of Water Quality: The Contribution of Advanced Technologies, *Elsevier,* Amsterdam, The Netherlands, 1998.
[9]. F. R. W. Trettnak, In Monitoring of Water Quality: The Contribution of Advanced Technologies, *Elsevier,* Amsterdam, The Netherlands, 1998.
[10].T.-C. D. C.-A. Opti-1 Terumo-Cardiovascular Devices CDI-2000 AVL Opti-1. Terumo-Cardiovascular Devices CDI-2000 AVL Opti-1.
[11].http://www.oceanoptics.com/products/sensors.asp
[12].P. E. Henning, A. Benko, A. W. Schwabacher, P. Geissinger, Apparatus and methods for optical time-of-flight discrimination in combinatorial library analysis, *Rev. Sci. Instr.,* Vol. 76, 2005, pp. 0622201-8.
[13].J. E. Lee, S. S. Saavedra, Evanescent sensing in doped sol-gel glass films, *Anal. Chim. Acta,* Vol. 285, 1994, pp. 265-269.
[14].B. D. MacCraith, G. O'Keeffe, C. McDonagh, A. K. McEvoy, LED-based fibre optic oxygen sensor using sol-gel coating, *Electron. Lett.,* Vol. 30, No. 11, 1994, pp. 888-889.
[15].B. D. MacCraith, Enhanced evanescent wave sensors using sol gel-derived porous glass coatings, *Sens. Actuators B Chem.,* Vol. 11, 1993, pp. 29-34.
[16].B. D. MacCraith, C. McDonagh, G. O'Keeffe, E. T. Keyes, J. G. Vos, B. O'Kelly, J. F. McGilp, Fibre optic oxygen sensor based on fluorescence quenching of evanescent-wave excited ruthenium complexes in sol gel-derived porous glass coating, *Analyst,* Vol. 118, 1993, pp. 385-388.

[17].B. D. MacCraith, B. D. MacCraith, V. Ruddy, C. Potter, B. O'Kelly, J. F. McGilp, Optical waveguide sensor using evanescent wave excitation of fluorescent dye in sol-gel glass, *Electron. Lett.,* Vol. 27, No. 14, 1991, pp. 1247-1248.
[18].B. J. Prince, N. T. Kaltcheva, A. W. Schwabacher, P. Geissinger, Fluorescent Fiber-Optic Sensor Arrays Probed Utilizing Evanescent Fiber-Fiber Coupling, *Appl. Spectrosc.,* Vol. 55, 2001, pp. 1018-1024.
[19].N. J. Harrick, Internal Reflection Spectroscopy, *Interscience Publishers*, New York, 1967.
[20].Y. Ueno, M. Shimizu, An optical-fiber cable fault location method, *IEEE J. Quantum Electron.,* Vol. 11, No. 9, 1975, pp. 899-900.
[21].Y. Ueno, M. Shimizu, Optical fiber fault location method, *Appl. Opt.,* Vol. 15, No. 6, 1976, pp. 1385-1388.
[22].S. D. Personick, Photon prove, an optical-fiber time-domain reflectometer, *Bell System Tech. J.,* Vol. 56, 1977, pp. 355-366.
[23].M. K. Barnoski, M. D. Rourke, S. M. Jensen, R. T. Melville, Optical time domain reflectometer, *Appl. Opt.,* Vol. 16, No. 9, 1977, pp. 2375-2379.
[24].R. A. Potyrailo, G. M. Hieftje, Optical Time-of-Flight Chemical Detection: Absorption-Modulated Fluorescence for Spatially Resolved Analyte Mapping in a Bidirectional Distributed Fiber-Optic Sensor, *Anal. Chem.,* Vol. 70, No. 16, 1998, pp. 3407-3412.
[25].B. J. Prince, A. W. Schwabacher, P. Geissinger, A Readout Scheme Providing High Spatial Resolution for Distributed Fluorescent Sensors on Optical Fibers, *Anal. Chem.,* Vol. 73, No. 5, 2001, pp. 1007-1015.
[26].J. R. Bacon, J. N. Demas, Determination of Oxygen Concentrations by Luminescence Quenching of a Polymer- Immobilized Transition-Metal Complex, *Anal. Chem.,* Vol. 59, 1987, pp. 2780-2785.
[27].D. B. Papkosky, New oxygen sensors and their application to biosensing, *Sens. Actuators B Chem.,* Vol. 29, 1995, pp. 213-218.
[28].J. R. Lakowicz, Principles of fluorescence spectroscopy, 3rd Edition, *Springer*, 2006.
[29].R. Banga, J. Yarwood, A. M. Morgan, B. Evans, J. Kells, FTIR and AFM Studies of the Kinetics and Self-Assembly of Alkyltrichlorosilanes and (Perfluoroalkyl)trichlorosilanes onto Glass and Silicon, *Langmuir,* Vol. 11, No. 11, 1995, pp. 4393-4399.
[30].P. Silberzan, L. Leger, D. Ausserre, J. J. Benattar, Silanation of silica surfaces. A new method of constructing pure or mixed monolayers, *Langmuir,* Vol. 7, No. 8, 1991, pp. 1647-1651.
[31].U. Abraham, Self-assembled monolayers of alkyltrichiorosilanes: Building blocks for future organic materials, *Adv. Mater.,* Vol. 2, No. 12, 1990, pp. 573-582.
[32].M. Lei, Y. Gu, A. Baldi, R. A. Siegel, B. Ziaie, High-Resolution Technique for Fabricating Environmentally Sensitive Hydrogel Microstructures, *Langmuir,* Vol. 20, No. 21, 2004, pp. 8947-8951.
[33].J. Z. Hilt, A. K. Gupta, R. Bashir, N. A. J. Peppas, Ultrasensitive Biomems Sensors Based on Microcantilevers Patterned with Environmentally Responsive Hydrogels, *Biomed. Microdevices,* Vol. 5, 2003, pp. 177-184.
[34].A. Revzin, R. J. Russell, V. K. Yadavalli, W.-G. Koh, C. Deister, D. D. Hile, M. B. Mellott, M. V. Pishko, Fabrication of Poly(ethylene glycol) Hydrogel Microstructures Using Photolithography, *Langmuir,* Vol. 17, No. 18, 2001, pp. 5440-5447.
[35].D. J. Beebe, J. S. Moore, J. M. Bauer, Q. Yu, R. H. Liu, C. Devadoss, B. H. Jo, Functional hydrogel structures for autonomous flow control inside microfluidic channels, *Nature,* Vol. 404, 2000, pp. 588-590.
[36].M. P. J. Hoffmann, D. Kuckling, W. Fischer, Photopatterning of thermally sensitive hydrogels useful for microactuators, *Sens. Actuators B Chem.,* Vol. 77, 1999, pp. 139-44.
[37].J. M. Kürner, I. Klimant, C. Krause, H. Preu, W. Kunz, O. S. Wolfbeis, Inert Phosphorescent Nanospheres as Markers for Optical Assays, *Bioconjugate Chem.,* Vol. 12, No. 6, 2001, pp. 883-889.
[38].R. A. Potyrailo, G. M. Hieftje, Oxygen detection by fluorescence quenching of tetraphenylporphyrin immobilized in the original cladding of an optical fiber, *Anal. Chim. Acta,* Vol. 370, 1998, pp. 1-8.
[39].A. Mills, Controlling the sensitivity of optical oxygen sensors, *Sens. Actuators B Chem.,* Vol. 51, No. 1-3, 1998, pp. 60-68.
[40].H. Y. Liu, S. C. Switalski, B. K. Coltrain, P. B. Merkel, Oxygen permeability of sol-gel coatings, *Appl. Spectrosc.,* Vol. 46, No. 8, 1988, pp. 1266-1272.
[41].X. M. Li, F. C. Ruan, K. Y. Wong, Optical characteristics of a ruthenium(II) complex immobilized in a silicone rubber film for oxygen measurement, *Analyst,* Vol. 118, No. 3, 1993, pp. 289 - 292.
[42].A. Mills, Q. Chang, Modelled diffusion-controlled response and recovery behavior of a naked optical film sensor with a hyperbolic-type response to analyte concentration, *Analyst,* Vol. 117, 1992, pp. 1461-1466.
[43].E. R. Carraway, J. N. Demas, B. A. DeGraff, Luminescence quenching mechanism for microheterogeneous systems, *Anal. Chem.,* Vol. 63, No. 4, 1991, pp. 332-336.

[44].J. N. Demas, B. A. DeGraff, W. Xu, Modeling of Luminescence Quenching-Based Sensors: Comparison of Multisite and Nonlinear Gas Solubility Models, *Anal. Chem.,* Vol. 67, No. 8, 1995, pp. 1377-1380.
[45].J. R. Lakowicz, G. Weber, Quenching of Fluorescence by Oxygen. A Probe for Structural Fluctuations in Macromolecules, *Biochemistry,* Vol. 12, No. 21, 1973, pp. 4161-4170.
[46].A. Mills, Response characteristics of optical sensors for oxygen: models based on a distribution in to or kq, *Analyst,* Vol. 124, 1999, pp. 1301-1307.
[47].W. Xu, K. A. Kneas, J. N. Demas, B. A. DeGraff, Oxygen Sensors Based on Luminescence Quenching of Metal Complexes: Osmium Complexes Suitable for Laser Diode Excitation, *Anal. Chem.,* Vol. 68, 1996, pp. 2605-2609.
[48].E. R. Carraway, J. N. Demas, B. A. DeGraff, J. R. Bacon, Photophysics and photochemistry of xygen sensors based on luminescent transition-metal complexes, *Anal. Chem.,* Vol. 63, No. 4, 1991, pp. 337-342.
[49].R. D. Bowman, K. A. Kneas, J. N. Demas, A. Periasamy, Conventional, confocal and two-photon fluorescence microscopy investigations of polymer-supported oxygen sensors, *J. Microscopy,* Vol. 211, No. 2, 2003, pp. 112-120.
[50].K. A. Kneas, J. N. Demas, B. A. DeGraff, A. Periasamy, Fluorescence Microscopy Study of Heterogeneity in Polymer-supported Luminescence-based Oxygen Sensors, *Microscopy and Microanalysis,* Vol. 6, No. 6, 2000, pp. 551-561.
[51].M. Z. B. Hoffman, F.; Moggi, L.; Hug, G. L. , Rate Constant for the Quenching of Excited States of Metal Complexes in Fluid Solution, *J. Phys. Chem. Ref. Data,* Vol. 18, 1989, pp. 219-543.
[52].M. E. Köse, B. F. Carroll, K. S. Schanze, Preparation and Spectroscopic Properties of Multiluminophore Luminescent Oxygen and Temperature Sensor Films, *Langmuir,* Vol. 21, No. 20, 2005, pp. 9121-9129.
[53].R. A. H. Potyrailo, Gary M., Oxygen detection by fluorescence quenching of tetraphenylporphyrin immobilized in the original cladding of an optical fiber, *Anal. Chim. Acta,* Vol. 370, No. 1, 1998, pp. 1-8.
[54].A. Mills, Q. Chang, Modelled diffusion-controlled response and recovery behavior of a naked optical film sensor with a hyperbolic-type response to analyte concentration, *Analyst,* Vol. 117, 1992, pp. 1461-1466.
[55].C. McDonagh, B. D. MacCraith, A. K. McEvoy, Tailoring of Sol-Gel Films for Optical Sensing of Oxygen in Gas and Aqueous Phase, *Anal. Chem.,* Vol. 70, No. 1, 1998, pp. 45-50.
[56].J. Coppeta, C. Rogers, Dual emission laser induced fluorescence for direct planar scalar behavior measurements, *Experiments in Fluids,* Vol. 25, No. 1, 1998, pp. 1-15.

Guide for Contributors

Aims and Scope

Sensors & Transducers Journal (ISSN 1726-5479) provides an advanced forum for the science and technology of physical, chemical sensors and biosensors. It publishes state-of-the-art reviews, regular research and application specific papers, short notes, letters to Editor and sensors related books reviews as well as academic, practical and commercial information of interest to its readership. Because it is an open access, peer review international journal, papers rapidly published in *Sensors & Transducers Journal* will receive a very high publicity. The journal is published monthly as twelve issues per annual by International Frequency Association (IFSA). In additional, some special sponsored and conference issues published annually. *Sensors & Transducers Journal* is indexed and abstracted very quickly by Chemical Abstracts, IndexCopernicus Journals Master List, Open J-Gate, Google Scholar, etc.

Topics Covered

Contributions are invited on all aspects of research, development and application of the science and technology of sensors, transducers and sensor instrumentations. Topics include, but are not restricted to:

- Physical, chemical and biosensors;
- Digital, frequency, period, duty-cycle, time interval, PWM, pulse number output sensors and transducers;
- Theory, principles, effects, design, standardization and modeling;
- Smart sensors and systems;
- Sensor instrumentation;
- Virtual instruments;
- Sensors interfaces, buses and networks;
- Signal processing;
- Frequency (period, duty-cycle)-to-digital converters, ADC;
- Technologies and materials;
- Nanosensors;
- Microsystems;
- Applications.

Submission of papers

Articles should be written in English. Authors are invited to submit by e-mail editor@sensorsportal.com 8-14 pages article (including abstract, illustrations (color or grayscale), photos and references) in both: MS Word (doc) and Acrobat (pdf) formats. Detailed preparation instructions, paper example and template of manuscript are available from the journal's webpage: http://www.sensorsportal.com/HTML/DIGEST/Submition.htm Authors must follow the instructions strictly when submitting their manuscripts.

Advertising Information

Advertising orders and enquires may be sent to sales@sensorsportal.com Please download also our media kit: http://www.sensorsportal.com/DOWNLOADS/Media_Kit_2009.pdf

Subscription 2010 is open!
SUBSCRIBE TODAY!

Sensors & Transducers Journal provides an advanced forum for the science and technology of physical, chemical sensors and biosensors. It publishes reviews, regular research and application specific papers and short notes. This peer reviewed international journal is indexed and abstracted very quickly by Chemical Abstracts, IndexCopernicus Journals Master List (ICV=6.31 at the end of 2008), Open J-Gate, Google Scholar, Scirus, etc.

Topics of Interest

Include, but are not restricted to:
Physical, chemical and biosensors
Digital, frequency, period, duty-cycle, pulse number output sensors and transducers
Theory, principles, effects, design, standardization and modelling
Smart sensors and systems
Sensor instrumentation
Virtual instruments
Sensors interfaces, buses and networks
Signal processing
Technologies and materials
Nanosensors
Microsystems
Applications

2008
e-Impact Factor
205.767

IFSA
www.sensorsportal.com

editor@sensorsportal.com
http://www.sensorsportal.com/HTML/DIGEST/Journal_Subscription_2010.htm

www.sensorsportal.com